

Influence of pore size on the Knight shift in liquid tin and mercury in a confined geometry

This article has been downloaded from IOPscience. Please scroll down to see the full text article.

2007 J. Phys.: Condens. Matter 19 106217

(<http://iopscience.iop.org/0953-8984/19/10/106217>)

View [the table of contents for this issue](#), or go to the [journal homepage](#) for more

Download details:

IP Address: 129.252.86.83

The article was downloaded on 28/05/2010 at 16:30

Please note that [terms and conditions apply](#).

Influence of pore size on the Knight shift in liquid tin and mercury in a confined geometry

Cheng Tien¹, E V Charnaya^{1,2,4}, M K Lee¹ and Yu A Kumzerov³

¹ Department of Physics, National Cheng Kung University, Tainan 70101, Taiwan

² Institute of Physics, St Petersburg State University, St Petersburg, Petrodvorets, 198504, Russia

³ A F Ioffe Physico-Technical Institute, RAS, St Petersburg, 194021, Russia

E-mail: charnaya@mail.ncku.edu.tw

Received 28 November 2006, in final form 5 February 2007

Published 23 February 2007

Online at stacks.iop.org/JPhysCM/19/106217

Abstract

¹¹⁹Sn and ¹⁹⁹Hg NMR studies were carried out for metallic tin and mercury embedded in synthetic opals and porous glasses. The Knight shift for confined liquid tin and mercury was found to decrease monotonically with decreasing pore size, evidence for the reduction of electron susceptibility. Size-induced alterations in the Knight shift were more pronounced for confined mercury than for tin. The influence of pore filling on the NMR line shape and Knight shift was observed for tin within opal. The reasons for the decreasing Knight shift for liquid metals in a confined geometry are discussed. Correlations between the alteration in the Knight shift and atomic number are shown, the changes in fractional values of the Knight shift remaining almost identical.

1. Introduction

Composites consisting of nanoporous matrices filled with various materials, in particular with metals, are of increasing interest for fundamental and applied physics ([1, 2] and references therein). Such nanocomposites provide the opportunity to study size effects due to the small sizes of nanoparticles within pores. They are also considered to be promising for technical applications because of two major advantages of confined geometry. The advantages are screening of particles in pores from harmful environments and fabrication of particle arrays of well defined geometry. Until now, different experimental techniques have been used to study the properties of liquid and solid metals within nanopores, including calorimetry, x-ray diffraction, magnetometry, acoustic methods and NMR (see [3–9] and references therein). Closest attention has been focused on the melting and freezing phase transitions and on properties of solid metallic nanoparticles embedded into pores. Confined liquid metals have been much less studied.

⁴ Author to whom any correspondence should be addressed.

NMR is an extremely powerful method for studying metals in confined geometry because of its high sensitivity to local structure, chemical bonding and atomic mobility. In particular, the Knight shift of the NMR line in metals is directly related to the electron susceptibility [10]. However, the influence of confinement on the Knight shift in liquid metals has only been observed for liquid gallium in porous glasses and opals [11] and for liquid indium in a porous glass [12]. While tin and mercury are commonly used metals in technical applications, size-effects on their electronic properties in the liquid state have not been studied until now. In the present paper ^{119}Sn and ^{199}Hg NMR was applied to measurements of the Knight shift and line shape for liquid metallic tin and mercury confined within porous matrices (synthetic opals and porous glasses).

2. Experimental details

The NMR measurements of confined liquid metallic tin and mercury were carried out using a Bruker Avance 400 pulse spectrometer in a magnetic field of 9.4 T. Tin has three naturally occurring isotopes the nuclei of which have non-zero magnetic moments. All three isotopes have spin $I = 1/2$ and therefore their quadrupole moment is equal to zero. Among them the isotope ^{119}Sn shows the best NMR signals and was chosen for measurements in the present paper. Its natural abundance is 8.59%. Mercury has two naturally occurring isotopes with non-zero magnetic moments, the isotope ^{199}Hg being better for NMR. Its natural abundance is 16.87% and its spin as for ^{119}Sn is $1/2$.

The ^{119}Sn and ^{199}Hg NMR line shape and Knight shift were measured for confined liquid tin and mercury using a single pulse sequence with phase cycling at 500 and 295 K, respectively. The temperature of measurements for tin was below the bulk tin melting point of 505 K since the melting and freezing phase transitions in confined tin were depressed noticeably compared to bulk in agreement with data for melting in isolated or supported tin particles [13–15]. Melting of confined mercury was also shifted to low temperatures compared to its bulk melting point of 234.3 K [6]. Thus, tin and mercury were completely melted within porous matrices under study at 500 and 295 K, respectively. The repetition time was 0.2 s. The NMR signals from ^{119}Sn and ^{199}Hg were rather weak because of the low natural abundance of the isotopes, so the necessary number of scans in our experiments varied from 4 to 40 000. The Knight shifts for confined tin and mercury were referenced to the signals from relevant bulk liquid metals.

Synthetic opals and porous glasses were used as porous matrices for tin and mercury. Opal consisted of close packed silica spheres of 210 nm in diameter. (More details about synthetic opals can be found in [16] and references therein.) Such an ideal structure should have octahedral and tetrahedral pores between adjacent spheres with radii of $r_1 = 0.414R$ and $r_2 = 0.224R$, respectively. Here R is the radius of the constituent silica spheres. The number of tetrahedral pores is twice the number of octahedral ones. Mercury intrusion porosimetry for the opal sample under study revealed two kinds of pores as expected with somewhat smaller radii— $r_1 \cong 30$ and $r_2 \cong 18$ nm. The overall volume of the two kinds of pores was about 0.9 of the total pore volume, the total relative volumes of tetrahedral and octahedral pores being the same. The remaining pore volume was occupied by fine pores with a radius of less than 2 nm. The porous glass which was filled with tin was prepared from phase-separated soda borosilicate glass by acid leaching. The main pore radius, 4 nm, was also determined using mercury intrusion porosimetry. This pore size corresponded to 93% of the total pore volume. The rest of the pore volume was occupied by pores with radii of less than 1 nm. Mercury was introduced into Vycor glass supplied by Corning, Inc. According to mercury porosimetry, the main pore radius was 3 nm. Information about the samples under study is presented in table 1.

Table 1. Samples under study. r is the average pore radius. Δr shows the pore size distribution and corresponds to 85% of pores near the average radius r lying within the range $r \pm \Delta r$.

Matrix	Opal		Porous glass	Vycor
r (nm)	30	18	4	3
Δr (nm)	5	3	0.2	0.3
Metal	Hg, Sn		Sn	Hg

Liquid tin and mercury were embedded into the porous matrices under high pressure up to 10 kbar. After the pressure was removed, some amount of metal flowed out of the pores. The tin filling factors, evaluated by weighing the samples after cooling down to room temperature, were 85 and 75% for the opal and glass, respectively. Since liquid tin, like mercury, does not wet the silica surface [17], it gathers into bigger pores under conditions of incomplete filling. Therefore, when the filling factor for the opal is 85%, almost all octahedral pores (about 45% of the total pore volume according to the mercury porosimetry) and some of tetrahedral pores (about 40% of the total pore volume) are filled with tin. Following the repetitive warming and cooling of the opal, the confined tin gradually flowed out of pores. This led to a decrease in the filling factor. Thus, when the filling was less than 45%, all confined tin was expected to fill the larger octahedral pores. The filling by mercury was not complete either. Even immediately after the pressure was removed, the filling factors were about 55% and 50% for the opal and glass, respectively. When the samples were weighed before measurements, the filling factors reduced to 35% for the opal and 40% for the Vycor glass. Thus, all confined mercury in opal should be gathered within the octahedral pores. For the porous glasses all confined tin and mercury should be gathered within the 4 and 3 nm pores, respectively, independently of the pore filling factor.

In addition, ^{119}Sn and ^{199}Hg NMR spectra for bulk liquid tin and mercury were measured at 508 K and room temperature, respectively. The measurements were carried out on tin particles with size of about 0.5 mm wrapped up in Teflon tape and on mercury drops of about 0.1 mm in size dispersed in Vaseline oil.

3. Results

^{119}Sn and ^{199}Hg NMR spectra obtained for liquid tin and mercury within the porous matrices are shown in figures 1 and 2 along with those for the relevant bulk melts. The spectra for liquid tin within the opal porous matrix shown in figure 1 were taken at two different filling factors. The broader line was obtained when the filling factor was 85%. The second narrower NMR line was taken when the filling was 40% of the total pore volume. The ^{119}Sn NMR line for the porous glass in figure 1 was taken at 75% filling but it did not change noticeably in shape or position upon decreasing the filling factor through repetitive warming. ^{199}Hg lines in figure 2 were measured when the filling factors were 35 and 40% for the opal and glass, respectively, as was mentioned in section 2. Their shape and position did not change either upon decreasing the filling factor due to a gradual flow of mercury out of pores.

4. Discussion

Figures 1 and 2 show that NMR lines for liquid tin as well as for liquid mercury in porous matrices are shifted to low frequencies. The lines are also slightly broadened compared to those in bulk melts. The line shapes are Lorentzian for bulk melted tin and mercury, in agreement with

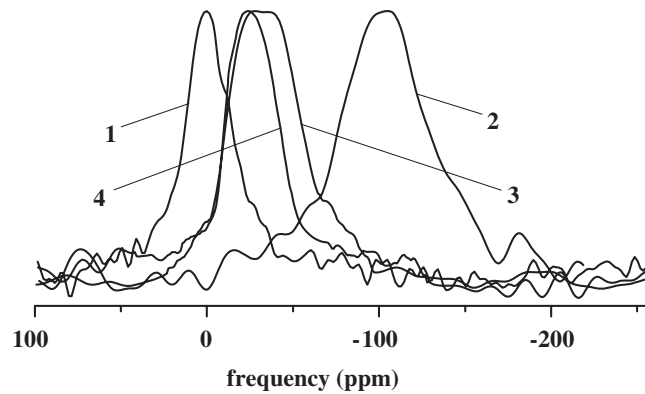


Figure 1. ^{119}Sn NMR lines for bulk liquid tin (1), liquid tin confined within porous glass (2) and opal with a filling factor of 85% (3) and 40% (4).

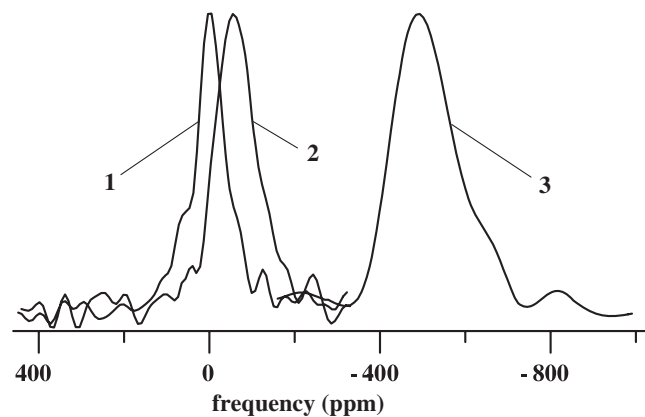


Figure 2. ^{199}Hg NMR lines for bulk liquid mercury (1) and for liquid mercury confined within opal (2) and Vycor glass (3).

previous NMR studies and theoretical predictions for liquid metals [18]. The line shapes for confined tin and mercury can be approximated with combinations of Lorentzian and Gaussian lines except for the ^{119}Sn line in the opal with 85% filling and a bimodal filled pore distribution. The Knight shift for them was measured as a position of the line peak relative to that for bulk melts and denoted below by ΔK . The ^{119}Sn and ^{199}Hg Knight shifts for tin and mercury embedded into opals at the 40% and 35% filling, respectively, obviously corresponded to metals within octahedral pores. The broader ^{119}Sn line for the opal at the 85% filling was treated by us as an overlap of two lines caused by tin in octahedral and tetrahedral pores in agreement with the bimodal distribution of filled pores at this filling factor. The Knight shifts for confined tin and mercury versus reciprocal pore radius are shown in figure 3. In figure 3 one can see the monotonic decrease in the Knight shift with decreasing pore size for both confined liquid tin and mercury, size-induced alterations in the Knight shift being more pronounced for mercury.

The Knight shift in liquid metals like tin and mercury with closed inner electron subshells originates mainly from the Fermi contact interaction of the spin polarized conduction electrons with nuclei (see [10, 18–21] and references therein):

$$K_s = \frac{8}{3}\pi \chi_s \Omega \langle |\Psi_F(0)|^2 \rangle, \quad (1)$$

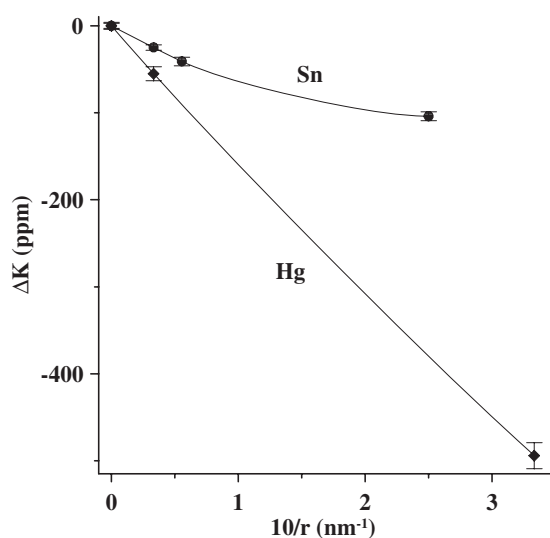


Figure 3. Dependence of the Knight shift ΔK relative to bulk on the inverse pore radius r for confined liquid tin (circles) and mercury (diamonds). The solid curves are guides for the eye.

where χ_s is the electron spin susceptibility per unit volume, Ω is the atomic volume and $\langle |\Psi_F(0)|^2 \rangle$ is the probability density at the nucleus of s-like electrons on the Fermi surface. The contributions from the orbital hyperfine interaction and core polarization [10] are small. Measurements on bulk liquid tin and mercury were consistent with theoretical examination and with spin–lattice relaxation studies. According to (1), the Knight shift caused by the contact interaction is directly proportional to the electron spin susceptibility.

Until now, the influence of particle size reduction on the Knight shift has been studied mostly for small isolated or supported metallic particles and thin layers in the solid state (see [22–25] and references therein). At low temperatures theories predict alterations in the Knight shift due to quantum size effects rising from increasing the separation of the conduction electron levels (see [26] and references therein). However, at higher temperatures the Knight shift could be affected chiefly by surface induced spatial variations in the density of electrons on the Fermi level which influence the total electron susceptibility because of the increased the surface to volume ratio (see [27] and references therein). The surface induced effects in the electron susceptibility depend on the electron structure of the metals under study. For transition metals the tight-binding approximation [27] predicts changes in the density of d-electrons near the surface which should lead to pronounced local shifts of NMR lines compared to bulk. The experimental results obtained for platinum and rhodium solid particles agree to a certain extent with this model [24].

According to theoretical calculations carried out using the local density functional formalism the spin susceptibility for simple metals with closed inner electron subshells should show damped Friedel oscillations near the metal surface; the integral surface magnetic susceptibility increases compared to bulk [27]. This model was applied to treat the strong broadening of NMR lines due to broad distribution in the Knight shift for small solid particles of such metals as Pb, Cu or Ag [24, 28]. The drastic resonance line broadening prevented clear observation of any size dependence of the Knight shift.

Contrary to the case of solid metals, the NMR lines for liquid nanoparticles should be narrowed due to atomic mobility. Thus, the Knight shift measured for confined liquid tin and

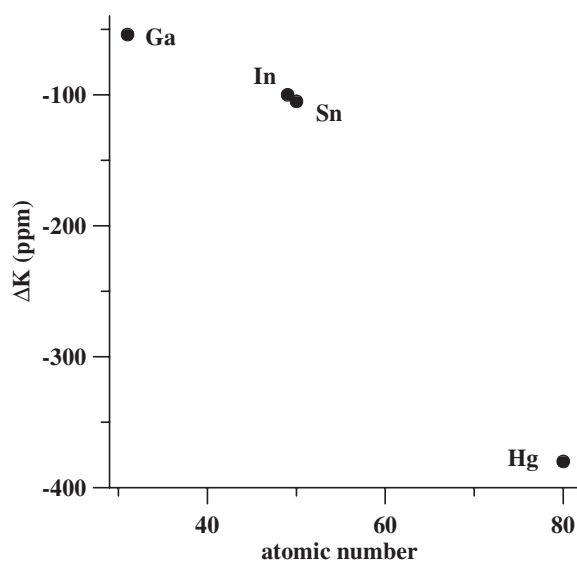


Figure 4. The change in the Knight shift relative to bulk for liquid tin, mercury, indium and gallium embedded into porous glass with 4 nm pore radius versus their atomic number. The value for gallium was taken from [11] and for indium from [12]. The Knight shift for confined mercury was estimated from the dependence on pore size in figure 3.

mercury nanoparticles should correspond to whole particles and the decrease in the Knight shift observed in the present studies reflects a size dependence of averaged values of the shift. According to (1) one should expect that the predicted enhancement of the integral surface electron susceptibility could lead to a total increase in the Knight shift for liquid nanoparticles of non-transition metals. However, the shift observed of ^{119}Sn and ^{199}Hg NMR lines for confined liquid tin and mercury to low frequencies contradicts these theoretical predictions. The decrease of the Knight shift cannot be explained either by the additional Laplace pressure which increases with decreasing sizes of small particles, since the Knight shift in bulk liquid mercury is known to increase with decreasing volume or increasing pressure [10, 18].

To reveal some regularities in the Knight shift alterations for confined liquid metals we collected NMR data in the plot of ΔK versus atomic number for liquid gallium, indium, tin and mercury embedded into porous glass with a 4 nm pore radius (figure 4). The Knight shift for gallium and indium was taken from [11] and [12], respectively. Data for tin and mercury are from the present study, the point for confined mercury taken from the dependence of the Knight shift on pore size shown in figure 3. One can see from figure 4 that the change in the Knight shift increases monotonically with increasing atomic number. However, since the Knight shift for bulk liquid metals, K_b , itself varies with atomic number [10] the fractional changes in the Knight shift under confinement, $\Delta K/K_b$, are more indicative. The fractional changes in the Knight shift corresponding to figure 4 are listed in table 2. One can see that the fraction $\Delta K/K_b$ is very similar for four melts and seems to be practically independent of atomic number. This result supports the suggestion that the confinement induced decrease in the Knight shift for liquid metals is mainly related to alterations in the electron spin susceptibility (in accordance with equation (1)) which in bulk depends only on the number of conduction electrons per unit volume within the framework of the free electron model [10].

The ^{119}Sn and ^{199}Hg NMR lines in confined melts were only slightly broadened compared to those in the relevant bulk (figures 1 and 2). The broadening is much less than was observed

Table 2. Fractional change in the Knight shift $\Delta K/K$ in liquid metals confined within porous glass with 4 nm pores and Knight shift K_b in bulk melts. Data for Sn and Hg are from the present study, those for Ga and In are taken from [11] and [12], respectively.

Metal	Sn	Hg	In	Ga
$\Delta K/K$ (%)	-1.43	-1.38	-1.26	-1.19
K_b (%)	0.73	2.74	0.79	0.45

for confined liquid gallium and indium where it was mostly induced by the quadrupolar contribution to spin relaxation [5, 12, 28, 29]. Since the Knight shift in confined tin and mercury was found here to depend on pore size, one can suggest that the NMR line broadening for tin and mercury under confinement compared to bulk is caused by the pore size distribution in the porous matrices. This agrees with the above mentioned admixture of Gaussian and Lorentzian line shapes for tin and mercury within pores and with the deconvolution of the ^{119}Sn line for the opal under the 85% filling factor resulting in two overlapped lines from tin confined within tetrahedral and octahedral pores.

In conclusion, ^{119}Sn and ^{199}Hg NMR measurements of the Knight shift and line shape were carried out on metallic tin and mercury embedded into nanoporous matrices to study effects induced by confinement. The Knight shift in liquid tin and mercury showed a monotonic decrease with decreasing pore size in contrast with theoretical predictions for electron spin susceptibility near the surface of metals with closed inner electron subshells. The decrease in the Knight shift for mercury was more pronounced compared with tin. The line broadening for confined liquid tin and mercury was attributed to the pore size distribution. The ^{119}Sn NMR line shape and shift for tin in opal were found to be sensitive to the filling factor due to the redistribution of tin over the pore volume.

Acknowledgment

The present work was supported by the Taiwan government under grant OUA 95-21T-2-017 and by RFBR (Russia).

References

- [1] Christenson H K 2001 *J. Phys.: Condens. Matter* **13** R95
- [2] Murray C B, Kagan C R and Bawendi M G 2000 *Annu. Rev. Mater. Sci.* **30** 545
- [3] Burchianti A, Bogi A, Marinelli C, Maibohm C, Mariotti E and Moi L 2006 *Phys. Rev. Lett.* **97** 157404
- [4] Xu Q *et al* 2006 *Phys. Rev. Lett.* **97** 155701
- [5] Charnaya E V, Loeser T, Michel D, Tien C, Yaskov D and Kumzerov Yu A 2002 *Phys. Rev. Lett.* **88** 097602
- [6] Borisov B F *et al* 1998 *Phys. Rev. B* **58** 5329
- [7] Unruh K M, Huber T E and Huber C A 1993 *Phys. Rev. B* **48** 9021
- [8] Charnaya E V, Tien C, Lin K J and Kumzerov Yu A 1998 *Phys. Rev. B* **58** 11089
- [9] Tien C, Charnaya E V, Wang W, Kumzerov Yu A and Michel D 2006 *Phys. Rev. B* **74** 024116
- [10] Carter G C, Bennett L H and Kahan D J 1977 *Metallic Shifts in NMR* (Oxford: Pergamon)
- [11] Charnaya E V, Michel D, Tien C, Kumzerov Yu A and Yaskov D 2003 *J. Phys.: Condens. Matter* **15** 5469
- [12] Charnaya E V, Tien C, Kumzerov Yu A and Fokin A V 2004 *Phys. Rev. B* **70** 052201
- [13] Bachelis T, Güntherodt H-J and Schäfer R 2000 *Phys. Rev. Lett.* **85** 1250
- [14] Lai S L, Guo J Y, Petrova V, Ramanath G and Allen L H 1996 *Phys. Rev. Lett.* **77** 99
- [15] Allen G L, Bayles R A, Gile W W and Jesser W A 1986 *Thin Solid Films* **144** 297
- [16] Lopez C 2003 *Adv. Mater.* **15** 1679
- [17] Amirfazli A, Chatain D and Neumann A W 1998 *Colloids Surf.* **142** 183
- [18] Titman J M 1977 *Phys. Rep.* **33** 1

- [19] Dickson E M 1969 *Phys. Rev.* **184** 294
- [20] Knight W D and Berger A G 1959 *Ann. Phys.* **8** 173
- [21] Havill R L 1967 *Proc. Phys. Soc.* **92** 945
- [22] Slichter C P 1999 *Phil. Mag.* B **79** 1253
- [23] Nagaev E L 1992 *Phys. Rep.* **222** 199
- [24] Van der Klink J J and Brom H B 2000 *Prog. Nucl. Magn. Reson. Spectrosc.* **36** 89
- [25] Vuissoz P-A, Ansermet J P and Wieckowski A 1999 *Phys. Rev. Lett.* **83** 2457
- [26] Kimura K 1990 *Phys. Rev. B* **42** 6939
- [27] Desjonqueres M C and Spanjaard D 1998 *Concepts in Surface Physics* (Berlin: Springer)
- [28] Williams M J, Edwards P P and Tunstall D P 1991 *Discuss. Faraday Soc.* **92** 199
- [29] Charnaya E V *et al* 2005 *Phys. Rev. B* **72** 035406